^{211}At Radioimmunotherapy of Subcutaneous Human Ovarian Cancer Xenografts: Evaluation of Relative Biologic Effectiveness of an α-Emitter In Vivo

Tom Bäck, BSc[1]; Håkan Andersson, MD, PhD[2]; Chaitanya R. Divgi, MD[3]; Ragnar Hultborn, MD, PhD[2]; Holger Jensen, PhD[4]; Sture Lindegren, PhD[1]; Stig Palm, PhD[1]; and Lars Jacobsson, PhD[1]

[1]Department of Radiation Physics, The Sahlgrenska Academy at Göteborg University, Göteborg, Sweden; [2]Department of Oncology, The Sahlgrenska Academy at Göteborg University, Göteborg, Sweden; [3]Department of Radiology, Memorial Sloan-Kettering Cancer Center, New York, New York; and [4]Positron Emission Tomography and Cyclotron Unit, Copenhagen, Denmark

The use of α-particle emitters in radioimmunotherapy (RIT) appears to be promising. We previously obtained convincing results in the treatment of microscopic intraperitoneal ovarian cancer in nude mice by using the α-emitter ^{211}At. This study was performed to evaluate the relative biological effectiveness (RBE) of ^{211}At compared with that of ^{60}Co γ-irradiation in an RIT model. Our endpoint was growth inhibition (GI) of subcutaneous xenografts. **Methods:** GI after irradiation was studied with subcutaneous xenografts of the human ovarian cancer cell line NIH: OVCAR-3 implanted in nude mice. The animals received an intravenous injection of ^{211}At-labeled monoclonal antibody MX35 F(ab′)$_2$ at different levels of radioactivity (0.33, 0.65, and 0.90 MBq). Control mice received unlabeled MX35 F(ab′)$_2$ only. To calculate the mean absorbed dose to tumor, a separate biodistribution study established the uptake of ^{211}At in tumors and organs at different times after injection. External irradiation of the tumors was performed with ^{60}Co. Tumor growth was monitored, and the normalized tumor volume (NTV) was calculated for each tumor. GI was defined by dividing the NTV values by the fitted NTV curve obtained from the corresponding control mice. To compare the biologic effects of the 2 radiation qualities, the mean value for GI (from day 8 to day 23) was plotted for each tumor as a function of its corresponding absorbed dose. From exponential fits of these curves, the doses required for a GI of 0.37 (D$_{37}$) were derived, and the RBE of ^{211}At was calculated. **Results:** The biodistribution study showed the uptake of the immunoconjugate by the tumor (amount of injected radioactivity per gram) to be 14% after 7 h. At 40 h, the ratio of uptake in tumors to uptake in blood reached a maximum value of 6.2. The administered activities of ^{211}At corresponded to doses absorbed by tumors of 1.35, 2.65, and 3.70 Gy. The value (mean ± SEM) for D$_{37}$ was 1.59 ± 0.08 Gy. Tumor growth after ^{60}Co external irradiation showed a value for D$_{37}$ of 7.65 ± 1.0 Gy. The corresponding RBE of ^{211}At irradiation was 4.8 ± 0.7. **Conclusion:** Using a tumor GI model in nude mice, we were able to derive an RBE of α-particle RIT with ^{211}At. The RBE was found to be 4.8 ± 0.7.

Key Words: astatine; radioimmunotherapy; relative biological effectiveness; xenografts

Interest in radioimmunotherapy (RIT) for various cancers is growing rapidly. The field was clinically established by the recent introduction of the first 2 U.S. Food and Drug Administration–approved drugs, ibritumomab tiuxetan (Zevalin; Biogen Idec Inc.) (1) and tositumomab (Bexxar; GlaxoSmithKline) (2), for the treatment of non-Hodgkin's lymphoma.

The development of strategies with different targeting agents, that is, antibodies and other ligands, continues. In the search for increased efficacy and lower toxicity for normal tissues, α-emitters may play an important role in the treatment of micrometastases and small tumors. Initial clinical trials have been carried out with the α-emitters ^{213}Bi (3) and ^{211}At (4).

Much effort has been devoted to determining the relative biological effectiveness (RBE) of α-particle irradiation and other types of high-LET (linear-energy-transfer) radiation. Most of these studies have focused on the effect on tumor cells in vitro, with various endpoints such as cell death and the induction of double strand breaks. Although a wide range of RBE (values of 2–20) has been proposed (5), a number in the interval from 3 to 5 is generally agreed on (6,7). Vandenbulcke et al. (8) compared the RBE of ^{213}Bi for tumor and nontumor cells by using an α-emitter RIT model in vitro, reporting values of 2–5, whereas Thomas et al. (9) reported a range of 10–13 for the lethality of ^{210}Po for bovine endothelial cells by using cellular damage endpoints. Reports on the RBE of α-radiation for tumors in vivo are

very limited, whereas for normal tissues there are some data. For example, Howell et al. reported values in the range of 3–9 for various α-particle emitters in their mouse testis model (10,11), and Elgqvist et al. (12) reported an RBE of 3.4–5 for myelotoxicity in nude mice after injection of [211]At-labeled antibodies. Behr et al. (13) reported values of 1–2 for myelotoxicity in mice. These data agree with data reported from clinical human studies with the α-emitter [213]Bi using the humanized murine monoclonal antibody (mAb) HuM195 (14).

Knowledge of the RBE for tumor cells is essential in the development and validation of tumor-seeking substances for therapy as well as for prediction of the therapeutic outcome in clinical practice. In combination with the RBE for normal tissues, it provides a tool with which α-particle radiation can be validated, in terms of the width of the therapeutic window. This window may be broader for high-LET radiation than for conventional low-LET radiation. Furthermore, this effect may be especially pronounced for cancer cells with low radiosensitivity.

In the present work, we sought a clinically relevant model for determination of the RBE in vivo of α-particle irradiation by using a human ovarian cancer cell line previously studied in vitro for determination of the RBE of [211]At (15). Subcutaneous tumors were established in nude mice, and tumor growth was monitored over time after treatment. The biologic endpoint used for calculations of the RBE was growth inhibition (GI). The reference low-LET irradiation was external ^{60}Co irradiation. A custom-built mouse cage ensured a homogeneous dose distribution within the tumors. Intravenously injected [211]At-labeled MX35 F(ab′)$_2$ fragments were used for α-particle irradiation. Dosimetry was based on separate experiments on tumor uptake at various times after injection.

MATERIALS AND METHODS

Production and Distillation of [211]At

[211]At, with a half-life of 7.2 h and α-particle energies of 5.9 (42%) and 7.5 (58%) MeV, was produced by irradiating a stable [209]Bi target at the cyclotron and PET unit, Rigshospitalet, Copenhagen, Denmark. The astatine, about 600 MBq, was isolated from the activated target by dry distillation as previously described (16), with a typical yield of 90%.

mAbs and Cell Lines

mAb MX35 recognizes a cell surface antigen, a glycoprotein of 95 kDa, expressed homogeneously on approximately 90% of human epithelial ovarian cancers (17). F(ab′)$_2$ fragments of mAb MX35 were kindly provided by K.O. Lloyd and C.R. Divgi at the Memorial Sloan–Kettering Cancer Center. The ovarian cancer cell line NIH:OVCAR-3 was obtained from the American Type Culture Collection and cultured at 37°C in cell culture medium (RPMI 1640 supplemented with 10% fetal calf serum, L-glutamine at 2 mmol/L, and 1% penicillin–streptomycin).

Radiolabeling with [211]At and Conjugation of Antibody

[211]At was coupled to MX35 F(ab′)$_2$ fragments by intermediate labeling with N-succinimidyl 3-(trimethylstannyl)benzoate (m-

MeATE). Conjugate labeling was performed as described previously (18), except that sodium ascorbate was introduced as a reducing agent after the labeling reaction. Briefly, 100 MBq of [211]At was oxidized in situ by N-iodosuccinimide and reacted with m-MeATE in methanol:1% acetic acid for 10 min. Sodium ascorbate (2.5 μmol) was added to the labeling mixture, and the methanol was evaporated. MX35 F(ab′)$_2$ fragments (150 μg) were added to the crude labeling residue, and conjugation was allowed to proceed for 20 min. The antibody fraction was finally isolated by passage over an NAP-5 column (Amersham Biosciences).

Immunoreactivity

The immunoreactivity of the radiolabeled mAb was analyzed in vitro by determination of the immunoreactive fraction. A fixed amount of antibody (10 ng in 0.040 mL of medium) was added to single-cell suspensions of NIH:OVCAR-3 in duplicate to a final volume of 0.540 mL. The cells were suspended in supplemented medium at 7 different concentrations, obtained by serial 1:2-fold dilutions, with resulting concentrations ranging from 5×10^6 to 0.078×10^6 cells per milliliter. After incubation with gentle agitation for 2 h at room temperature, the cells were centrifuged and rinsed twice in phosphate-buffered saline (PBS). Specific binding to the cells was determined by radioactivity measurements of the rinsed pellets in a γ-counter (Wizard 1480; Perkin–Elmer Life Sciences). Levels of the immunoreactive fraction, representing conditions of infinite antigen excess, were derived from a double-inverse plot of the total applied radioactivity divided by the cell-bound radioactivity as a function of the inverse of the cell concentration, as described by Lindmo et al. (19).

Tumors and Animals

Subcutaneously growing tumors were established as xenografts on female nude mice (BALB/c nu/nu; Charles River Breeding Laboratories) by inoculation of 2×10^7 NIH:OVCAR-3 cells in 0.4 mL of PBS. Each animal received 2 subcutaneous injections of cells in the scapula region at the age of 5–8 wk. Tumors were allowed to grow for 10–14 d, reaching a volume of approximately 100 mm³, at which point the irradiation procedure was performed. With a slide caliper, tumor volumes were determined by measurements of the larger tumor diameter (a) and the perpendicular diameter (b), from which the volume (V) was calculated with the following formula (20): $V = (a \times b^2)/2$.

This study was approved by the Ethics Committee for Animal Experiments of Göteborg University. The animals were fed ad libitum and housed according to directives of the Swedish Agency for Animal Welfare.

Irradiation with [211]At

Tumor irradiation with the high-LET α-emitter [211]At was performed systemically as RIT. The animals received a single injection in the tail vein of [211]At-labeled F(ab′)$_2$ fragments of mAb MX35 (3, 6, and 9 μg) in PBS (0.10 mL). The levels of radioactivity administered were 0.33, 0.65, and 0.90 MBq. Each radioactivity group included 7 animals (14 tumors), that is, 42 tumors in total. The animals in the nonirradiated control group received unlabeled antibody only (9 μg in 0.10 mL of PBS). This group included 8 animals (16 tumors).

Irradiation with [60]Co

Low-LET γ-irradiation of the tumors was performed as whole-body external ^{60}Co beam irradiation at a low dose rate. All animals in the same dose group were treated simultaneously. The animals

were placed in a plastic cage (polymethylmetaacrylate; 5-mm wall thickness to ensure a sufficient buildup area), wherein each animal was allowed to move freely in a separate corridor during irradiation. The center of each 3-cm-wide corridor was placed at a distance of 150 cm from the ^{60}Co radiation source. Six different absorbed doses to tumor, ranging from 1.4 to 5.8 Gy, were achieved by varying the time of irradiation (43–153 min). Each of the 6 dose groups included 7 animals (14 tumors), corresponding to 84 tumors in total. The 2 untreated control groups included 8 animals (16 tumors) each. The dose rate corresponding to the mean position of the animal during irradiation (~2 Gy/h) was checked by ion chamber measurements. The behavior and weight of the animals were unaffected by either irradiation procedure, except for 5 animals subjected to the highest level (5.8 Gy) of external ^{60}Co irradiation. These animals failed to maintain nutrition and were put to death at 11 d after treatment.

GI and RBE

Tumor growth was monitored by volume measurements every second day up to 60 d after treatment. The normalized tumor volume (NTV) was established from each tumor measurement by dividing the tumor volume on that day by its initial volume. The endpoint GI was defined by dividing the NTV for each tumor measurement within a treatment group by a value derived from an exponential fit of the NTV curve obtained from the corresponding control group.

Finally, to compare the biologic effects of the 2 radiation qualities, the mean value for GI (from day 8 to day 23) was plotted for each tumor as a function of its corresponding absorbed dose. From monoexponential fits of these curves, the absorbed doses required for a GI corresponding to 0.37 (D_{37}) were derived, and the RBE (37%) was calculated by dividing D_{37} for ^{60}Co by that for ^{211}At.

Biodistribution Study and Dosimetry

A separate in vivo biodistribution study was performed to estimate the mean absorbed dose to tumor for ^{211}At irradiation. This study was performed under the same conditions as those used in the GI study. Animals bearing tumors with a volume of approximately 100 mm^3 received an intravenous injection of radiolabeled (^{211}At, 0.56 MBq) antibody (MX35 F(ab$'$)$_2$, 11 μg) in 0.10 mL of PBS. The animals were sacrificed by cervical dislocation at various times after injection (0.5–45 h), and blood, organs, and tumors were removed. The tissues were weighed, and the radioactivity was measured (corrections were made for decay and background). From these data, mean concentrations of the radionuclide in tissues at various times after injection were calculated and related to the amount of injected radioactivity per gram (%IA/g). The mean values for %IA/g in the tumors at various times were used to calculate the cumulated activity concentration ($\tilde{C}$) for each tumor in the GI study. The mean absorbed dose to tumor (D) was calculated with the formula $D = \tilde{C} \times \Delta$, where Δ is the mean energy per decay.

RESULTS

Tumors and Animals

At 2 wk after cell inoculation, the mean tumor volume (mean $\pm$ SEM) in the ^{211}At irradiation groups was 44 $\pm$ 24 mm^3, whereas in the groups subjected to ^{60}Co irradiation, the mean tumor volume was 56 $\pm$ 23 mm^3. At dissection, all tumors in the biodistribution study appeared macroscopically homogeneous, with no signs of necrosis. When some of these tumors ($n = 10$) were divided into peripheral and central parts, γ-counting did not reveal any significant differences (less than 20%) in the uptake of the ^{211}At-labeled antibody within these tumor parts.

The behavior and weight of the animals were unaffected by the irradiation procedures, apart from 5 animals subjected to the highest level (5.8 Gy) of external ^{60}Co irradiation. These animals failed to maintain nutrition and were put to death at the first sign of abnormal behavior.

Radiolabeling and Immunoreactivity of Antibody

Radiolabeling with ^{211}At and subsequent antibody conjugation were performed by the m-MeATE method, with total yields of 30%–35%. Radiochemical analysis by methanol precipitation showed a protein-bound fraction of 0.95–0.98. The immunoreactive fraction of the radiolabeled antibody in NIH:OVCAR-3 cells was found to be >0.85 for all preparations used in this study.

Biodistribution Study and Dosimetry

Clearance of the immunoconjugate from the circulation showed an initial half-life of ~4 h. At 40 h after injection, less than 1 %IA/g was detected in the blood. The uptake in the tumor was 10 %IA/g at 10 h after injection, after which the concentration was maintained until 21 h after injection. The uptake reached a maximum at 7–9 h after injection, at 14 %IA/g, followed by a decrease corresponding to a biologic half-life of about 10 h (Fig. 1A). No statistical correlation was found between tumor uptake (%IA/g) and tumor weight.

When analyzed in relation to blood content (Fig. 1B), the ratio of uptake in tumors to uptake in blood showed a linear increase, reaching a level of 1.0 at 6 h after injection and reaching a maximum level (6.2) at 40 h after injection. Table 1 summarizes the biodistribution data for the analyzed tissues. The uptake in organs was in general low. As is often observed for astatine-labeled substances (21), some organs showed an uptake greater than the general extracellular distribution. This finding was most significant for the thyroid (throat), stomach, lungs, and salivary glands.

Using the tumor uptake (%IA/g at various hours after injection) obtained from the biodistribution study, the mean absorbed doses to tumor were calculated for each level of radioactivity administered in the GI study. The injected amounts of 0.33, 0.65, and 0.90 MBq of ^{211}At corresponded to mean absorbed doses to tumor of 1.35, 2.65, and 3.70 Gy, respectively.

GI After Internal Irradiation with ^{211}At

After intravenous injection of the immunoconjugate at 3 levels of radioactivity, the inhibition of tumor growth after treatment was studied by volume measurements. The NTV was calculated for each group and plotted versus time. As shown in Figure 2, the untreated control tumors showed clear exponential growth, whereas those irradiated showed
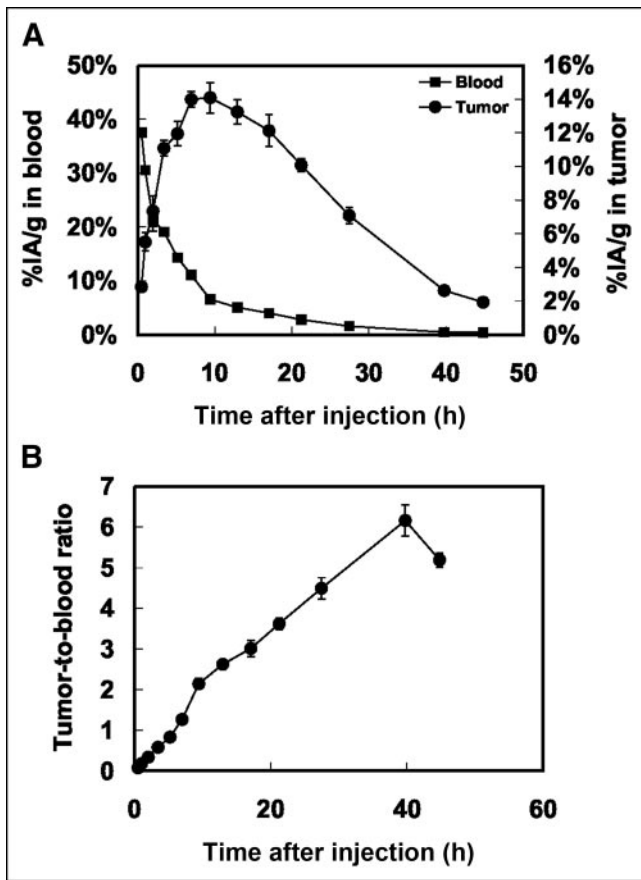
FIGURE 1. (A) Blood clearance and tumor uptake of ^{211}At-labeled MX35 F(ab')$_2$ in biodistribution study. %IA/g is shown as function of time after injection. (B) Ratio of uptake in tumors to uptake in blood (tumor-to-blood ratio) as function of time after injection. Data are given as mean ± SEM.

dose-dependent inhibition. The individual GI values (mean from day 8 to day 23) plotted as a function of the absorbed doses from ^{211}At yielded a D_{37} value of 1.59 ± 0.08 Gy, when an exponential fit was used (Fig. 3).

GI After External Irradiation with ^{60}Co

Figure 4 shows tumor growth after external irradiation with ^{60}Co, which was performed on 2 different occasions. The D_{37} value after ^{60}Co irradiation was 7.65 ± 1.0 Gy, when derived from an exponential fit of the plot of individual tumor GI values (mean from day 8 to day 23) as a function of the corresponding absorbed doses (Fig. 3).

RBE of ^{211}At In Vivo

The RBE, calculated as the ratio of the D_{37} values given above for ^{60}Co and ^{211}At, was 4.8 ± 0.7. This value is based on the mean value of GI from day 8 to day 23. Calculations of the RBE based on GI data at 2-d intervals, between day 8 and day 23, showed a moderate variation (3.6–6.3), with a mean value of 5.0 (Fig. 5).

DISCUSSION

Absorbed dose estimations are routinely used for planning and evaluation of external radiation therapy but are

TABLE 1
Biodistribution of ^{211}At-Labeled MX35 F(Ab')$_2$ in Nude Mice

| Sample	Mean ± SEM* %IA/g at following time after injection (h):										
	0.5	1.0	2.0	3.4	5.2	7.0	9.4	12.9	17.0	21.2	27.4
Blood	37.5 ± 0.7	30.5 ± 0.3	21.2 ± 2.0	19.1 ± 0.7	14.3 ± 0.4	11.1 ± 0.1	6.6 ± 0.3	5.0 ± 0.2	4.0 ± 0.1	2.8 ± 0.1	1.6 ± 0.0
Salivary glands	3.0 ± 0.3	3.9 ± 0.3	5.3 ± 0.5	7.9 ± 0.2	8.1 ± 0.5	8.2 ± 1.7	6.0 ± 0.7	10.3 ± 3.1	10.7 ± 0.8	7.0 ± 1.1	3.6 ± 0.5
Throat	5.6 ± 0.2	11.6 ± 1.6	16.2 ± 3.2	36.9 ± 4.6	23.7 ± 1.5	27.6 ± 5.6	24.0 ± 5.4	39.2 ± 3.7	40.5 ± 8.9	33.9 ± 3.3	32.0 ± 5.1
Lungs	13.4 ± 1.0	11.9 ± 0.3	11.5 ± 1.6	12.3 ± 0.8	10.4 ± 0.5	8.8 ± 0.3	6.1 ± 0.3	6.2 ± 0.2	6.6 ± 0.7	5.3 ± 0.1	3.8 ± 0.2
Heart	10.7 ± 0.7	10.0 ± 0.6	7.8 ± 1.1	8.1 ± 0.6	5.8 ± 0.1	5.1 ± 0.2	3.0 ± 0.1	2.5 ± 0.1	2.6 ± 0.2	2.0 ± 0.2	1.3 ± 0.0
Stomach	4.5 ± 0.7	4.4 ± 0.4	6.0 ± 1.1	12.3 ± 1.0	8.3 ± 0.2	7.5 ± 0.3	7.0 ± 1.4	6.5 ± 0.5	6.4 ± 0.2	7.4 ± 0.4	6.3 ± 0.6
Small intestine	5.6 ± 0.5	5.5 ± 1.0	4.3 ± 0.5	4.5 ± 0.4	3.1 ± 0.1	2.6 ± 0.3	1.7 ± 0.1	1.7 ± 0.2	2.0 ± 0.2	1.5 ± 0.1	1.2 ± 0.1
Large intestine	2.2 ± 0.1	2.5 ± 0.2	2.7 ± 0.4	3.1 ± 0.1	2.5 ± 0.2	1.8 ± 0.0	1.7 ± 0.1	1.2 ± 0.1	1.4 ± 0.1	1.2 ± 0.1	0.8 ± 0.0
Liver	8.3 ± 0.3	6.8 ± 0.4	5.0 ± 0.6	4.8 ± 0.2	3.2 ± 0.1	2.8 ± 0.2	1.6 ± 0.1	1.3 ± 0.1	1.3 ± 0.1	0.9 ± 0.0	0.7 ± 0.0
Spleen	8.7 ± 0.4	6.1 ± 0.2	5.0 ± 0.7	5.0 ± 0.2	4.6 ± 0.2	4.1 ± 0.1	2.8 ± 0.3	2.6 ± 0.1	2.7 ± 0.5	1.7 ± 0.1	1.4 ± 0.1
Kidneys	19.6 ± 0.7	21.4 ± 1.3	18.6 ± 0.9	16.0 ± 0.8	11.4 ± 0.1	9.3 ± 0.1	5.5 ± 0.3	4.7 ± 0.2	4.0 ± 0.1	2.7 ± 0.1	1.9 ± 0.1
Intraperitoneal fat	3.1 ± 0.4	2.8 ± 0.1	2.8 ± 1.0	2.7 ± 0.3	2.0 ± 0.2	1.9 ± 0.1	1.3 ± 0.1	1.5 ± 0.2	1.4 ± 0.1	1.2 ± 0.1	0.7 ± 0.1
Muscle	2.0 ± 0.9	1.5 ± 0.1	1.3 ± 0.2	1.5 ± 0.1	1.4 ± 0.1	1.2 ± 0.0	0.8 ± 0.0	0.9 ± 0.1	0.8 ± 0.1	0.7 ± 0.0	0.4 ± 0.0
Tumor	2.8 ± 0.1	5.5 ± 0.5	7.3 ± 0.8	11.1 ± 0.5	11.9 ± 0.7	14.0 ± 0.5	14.1 ± 0.9	13.2 ± 0.7	12.1 ± 0.9	10.1 ± 0.4	7.1 ± 0.5

*$n = 3$ for all time points.
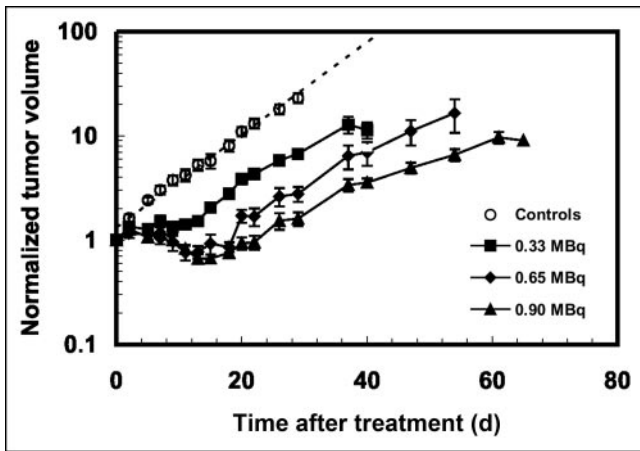
FIGURE 2. Tumor growth after internal irradiation with [211]At-labeled MX35 F(Ab′)$_2$ at 3 levels of radioactivity. NTV is shown as function of time after treatment. Dashed line represents exponential fit of control group. Data are given as mean ± SEM.
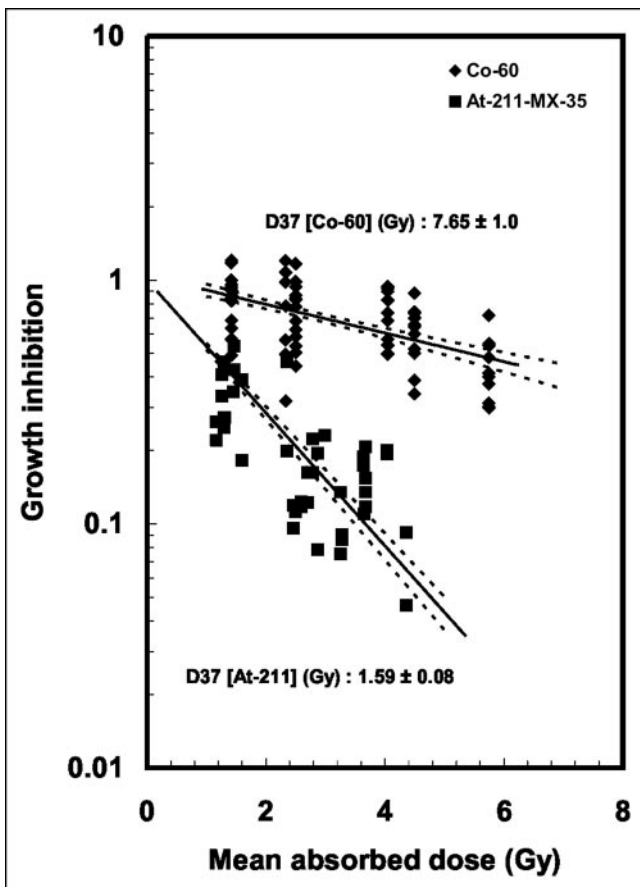

FIGURE 3. GI for 2 radiation qualities. Mean value (from day 8 to day 23) of GI for each tumor as function of its corresponding mean absorbed dose is shown. Solid lines represent monoexponential fits from which absorbed doses required for D$_{37}$ were derived. For [211]At irradiation, extrapolation number was 1.04; for ^{60}Co, extrapolation number was forced to 1.0. Dashed lines indicate 67% confidence limits for regression fit.
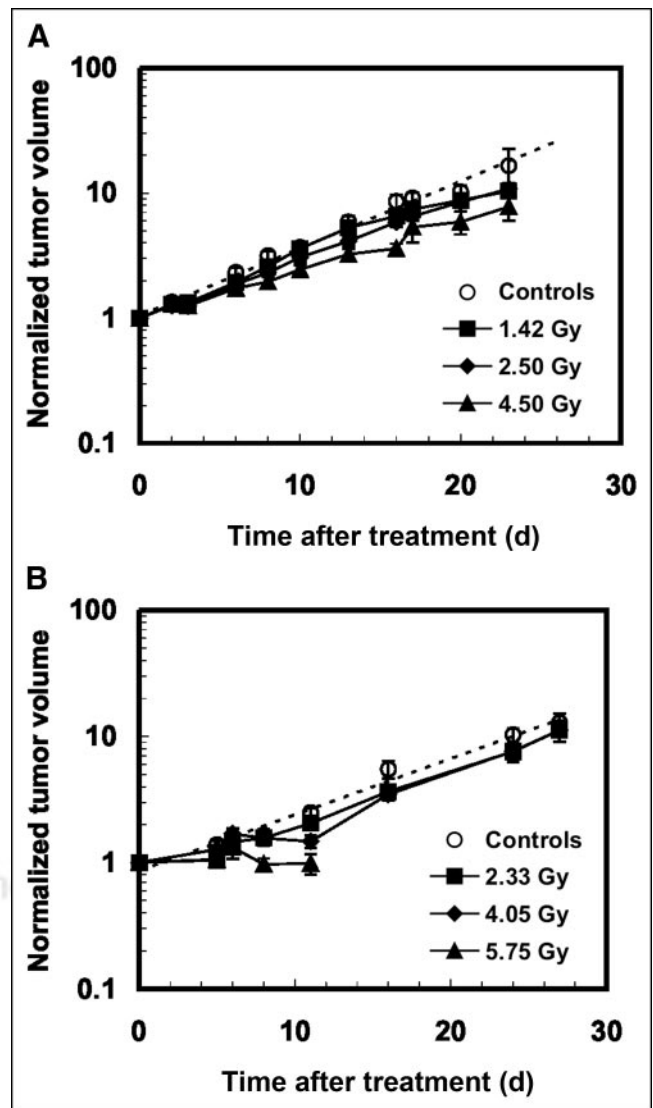

FIGURE 4. Tumor growth after external irradiation with [60]Co. NTV is shown as function of time after treatment. Irradiation was performed on 2 different occasions (A and B), each with its own corresponding control group. Data are given as mean ± SEM.

also strongly recommended for internal radionuclide therapy. For low-LET radiation, there is a great deal of clinical experience of tumor response and normal tissue toxicity at various dose levels, making the absorbed dose concept clinically relevant. However, for high-LET radiation, clinical experience so far is very limited. The biologic effectiveness in vivo, expressed as the RBE, has not been thoroughly studied for any high-LET radiation. Behr et al. found an RBE value of 2–3 with respect to antitumor efficacy in a xenograft model (*22*). In vitro studies have shown RBE values ranging from 2 to 10 for high-LET radiation (*23–25*). In the context of radiation protection, a radiation weighting factor of 20 is used, but this value is based on estimations of the risk of carcinogenesis. A recent study with [211]At RIT in nude mice showed an RBE of 3.4–5 for myelotoxicity (*12*). The value of 4.8 ± 0.7 for tumors presented here would
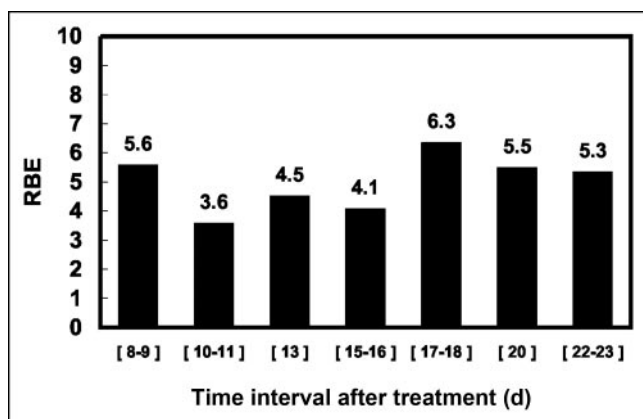
FIGURE 5. Variation in RBE over time when derived from GI data at 1- or 2-d intervals, between day 8 and day 23 after treatment.

imply no extra gain in the therapeutic window by use of high-LET radiation, because the enhancement of therapeutic efficacy is similar to that of toxicity. Even so, there are potential advantages of using high-LET radiation, in that the dependency of hypoxia and cell cycle phase on cell survival is much smaller than that for low-LET radiation (26).

We previously studied the effect of ^{211}At RIT on microscopic tumors of ovarian cancer in the peritoneal cavity (27). Although clinically relevant, that model is not useful for RBE studies because of difficulties in observing tumor development and estimating the absorbed dose to tumor. The macroscopic subcutaneous tumor model used in this study makes it possible to quantify tumor GI and to correlate this quantity to absorbed dose. A therapeutic disadvantage of this model is the slow diffusion of the immunoconjugate into the macroscopic tumor. The maximum achievable absorbed dose to tumor is limited because of the moderate ratio of uptake in tumors to uptake in blood achieved during the time of irradiation ($\approx$24 h). The slow diffusion in combination with the short particle range also may result in a heterogeneous dose distribution, reducing the overall tumor cell eradication effect.

Although the microdistribution of doses within the tumors was not determined in this work, the tumors seemed to be macroscopically homogeneous at dissection, with no signs of necrosis. This finding was supported by the fact that when tumors were divided into peripheral and central parts, no significant differences in the uptake of the ^{211}At-labeled antibody could be detected by γ-counting of these samples. Despite the fact that this study did not include any analysis of the distribution of the radiopharmaceutical compound at the cellular level, it seems reasonable to assume from our data that substantial amounts of the antibody complex did indeed reach the antigen target on tumor cells. Some of the complex also would have been in the vicinity of the cells while diffusing through the extracellular matrix or while present in the intratumoral capillaries. Taking into account

the distances (capillary to tumor cell) generally relevant for tumors (0–100 μm) (28–30) and the range of α-particles ($\sim$60 μm), decays in the vicinity of the tumor cells also would have contributed to cell irradiation. However, the dose distribution at the cellular level was almost certainly rather nonhomogeneous, resulting in a lower level of cell death. This, in turn, would imply an RBE higher than that presented here.

Even though the dose rate for ^{60}Co irradiation was kept low (2 Gy/h), it was not possible in this study to mimic the dose rate pattern of ^{211}At irradiation. The possibility that this factor would influence the RBE cannot be excluded.

CONCLUSION

The RBE for ^{211}At α-particle irradiation was derived on the macroscopic scale for solid tumors in vivo. Through the use of a tumor GI model and low-dose-rate ^{60}Co γ-irradiation for comparison, the RBE was found to be 4.8 ± 0.7.

REFERENCES

1. Ibritumomab tiuxetan (Zevalin) for non-Hodgkin's lymphoma. *Med Lett Drugs Ther*. 2002;44:101–102.
2. Iodine-131 tositumomab (Bexxar) for treatment of lymphoma. *Med Lett Drugs Ther*. 2003;45:86–87.
3. Jurcic JG, Larson SM, Sgouros G, et al. Targeted alpha particle immunotherapy for myeloid leukemia. *Blood*. 2002;100:1233–1239.
4. Zalutsky MR. Current status of therapy of solid tumors: brain tumor therapy. *J Nucl Med*. 2005;46(suppl 1):151S–156S.
5. Barendsen GW. The relationships between RBE and LET for different types of lethal damage in mammalian cells: biophysical and molecular mechanisms. *Radiat Res*. 1994;139:257–270.
6. Ballangrud AM, Yang WH, Charlton DE, et al. Response of LNCaP spheroids after treatment with an alpha-particle emitter (^{213}Bi)-labeled anti-prostate-specific membrane antigen antibody (J591). *Cancer Res*. 2001;61:2008–2014.
7. Aurlien E, Larsen RH, Akabani G, et al. Exposure of human osteosarcoma and bone marrow cells to tumour-targeted alpha-particles and gamma-irradiation: analysis of cell survival and microdosimetry. *Int J Radiat Biol*. 2000;76:1129–1141.
8. Vandenbulcke K, De Vos F, Offner F, et al. In vitro evaluation of ^{213}Bi-rituximab versus external gamma irradiation for the treatment of B-CLL patients: relative biological efficacy with respect to apoptosis induction and chromosomal damage. *Eur J Nucl Med Mol Imaging*. 2003;30:1357–1364.
9. Thomas PA, Tracy BL, Ping T, et al. Relative biological effectiveness (RBE) of ^{210}Po alpha-particles versus x-rays on lethality in bovine endothelial cells. *Int J Radiat Biol*. 2003;79:107–118.
10. Howell RW, Azure MT, Narra VR, Rao DV. Relative biological effectiveness of alpha-particle emitters in vivo at low doses. *Radiat Res*. 1994;137:352–360.
11. Howell RW, Goddu SM, Narra VR, et al. Radiotoxicity of gadolinium-148 and radium-223 in mouse testes: relative biological effectiveness of alpha-particle emitters in vivo. *Radiat Res*. 1997;147:342–348.
12. Elgqvist J, Bernhardt P, Hultborn R, et al. Myelotoxicity and RBE of ^{211}At-conjugated monoclonal antibodies compared with ^{99m}Tc-conjugated monoclonal antibodies and ^{60}Co irradiation in nude mice. *J Nucl Med*. 2005;46:464–471.
13. Behr TM, Behe M, Sgouros G. Correlation of red marrow radiation dosimetry with myelotoxicity: empirical factors influencing the radiation-induced myelo-

toxicity of radiolabeled antibodies, fragments and peptides in pre-clinical and clinical settings. *Cancer Biother Radiopharm*. 2002;17:445–464.

14. Sgouros G, Ballangrud AM, Hamacher KA, et al. β- vs. α-Emitter dose-response analysis in patients [abstract]. *J Nucl Med*. 2000;41(suppl):82P.

15. Palm S, Andersson H, Back T, et al. In vitro effects of free [211]At,[211]At-albumin and [211]At-monoclonal antibody compared to external photon irradiation on two human cancer cell lines. *Anticancer Res*. 2000;20:1005–1012.

16. Lindegren S, Back T, Jensen HJ. Dry-distillation of astatine-211 from irradiated bismuth targets: a time-saving procedure with high recovery yields. *Appl Radiat Isot*. 2001;55:157–160.

17. Welshinger M, Yin BW, Lloyd KO. Initial immunochemical characterization of MX35 ovarian cancer antigen. *Gynecol Oncol*. 1997;67:188–192.

18. Lindegren S, Andersson H, Back T, et al. High-efficiency astatination of antibodies using N-iodosuccinimide as the oxidising agent in labelling of N-succinimidyl 3-(trimethylstannyl)benzoate. *Nucl Med Biol*. 2001;28:33–39.

19. Lindmo T, Boven E, Cuttitta F, Fedorko J, Bunn PA Jr. Determination of the immunoreactive fraction of radiolabeled monoclonal antibodies by linear extrapolation to binding at infinite antigen excess. *J Immunol Methods*. 1984;72:77–89.

20. Carlsson G, Gullberg B, Hafstrom L. Estimation of liver tumor volume using different formulas: an experimental study in rats. *J Cancer Res Clin Oncol*. 1983;105:20–23.

21. Larsen RH, Slade S, Zalutsky MR. Blocking [[211]At]Astatide accumulation in normal tissues: preliminary evaluation of seven potential compounds. *Nucl Med Biol*. 1998;25:351–357.

22. Behr TM, Behe M, Stabin MG, et al. High-linear energy transfer (LET) alpha versus low-LET beta emitters in radioimmunotherapy of solid tumors: therapeutic

23. efficacy and dose-limiting toxicity of [213]Bi- versus ^{90}Y-labeled CO17-1A Fab′ fragments in a human colonic cancer model. *Cancer Res*. 1999;59:2635–2643.

23. Barendsen GW. RBE for non-stochastic effects. *Adv Space Res*. 1992;12:385–392.

24. Persson LM, Edgren MR, Stenerlow B, et al. Relative biological effectiveness of boron ions on human melanoma cells. *Int J Radiat Biol*. 2002;78:743–748.

25. Neti PV, de Toledo SM, Perumal V, Azzam EI, Howell RW. A multi-port low-fluence alpha-particle irradiator: fabrication, testing and benchmark radiobiological studies. *Radiat Res*. 2004;161:732–738.

26. Auberger T, Thurriegl B, Freude T, et al. Oxygen tension in transplanted mouse osteosarcomas during fractionated high-LET and low-LET radiotherapy: predictive aspects for choosing beam quality? *Strahlenther Onkol*. 1999;175(suppl 2):52–56.

27. Andersson H, Palm S, Lindegren S, et al. Comparison of the therapeutic efficacy of [211]At- and ^{131}I-labelled monoclonal antibody MOv18 in nude mice with intraperitoneal growth of human ovarian cancer. *Anticancer Res*. 2001;21:409–412.

28. Folkman J. Can mosaic tumor vessels facilitate molecular diagnosis of cancer? *Proc Natl Acad Sci USA*. 2001;98:398–400.

29. Konerding MA, Miodonski AJ, Lametschwandtner A. Microvascular corrosion casting in the study of tumor vascularity: a review. *Scanning Microsc*. 1995;9:1233–1243.

30. Lauk S, Zietman A, Skates S, Fabian R, Suit HD. Comparative morphometric study of tumor vasculature in human squamous cell carcinomas and their xenotransplants in athymic nude mice. *Cancer Res*. 1989;49:4557–4561.